Sensors & Actuators: B. Chemical 368 (2022) 132180

Contents lists available at ScienceDirect

Sensors and Actuators: B. Chemical

journal homepage: www.elsevier.com/locate/snb

Rapid warning microanalyzer for heavy metals monitoring in natural waters

Alex Pascual-Esco , Julián Alonso-Chamarro , Mar Puyol *

Group of Sensors and Biosensors, Department of Chemistry, Faculty of Sciences, Universitat Autònoma de Barcelona, Carrer dels Til·lers s/n, Bellaterra, 08193 Cerdanyola del Vallès, Spain

ARTICLE INFO

Keywords:
Carbon Dots
Heavy metals
Fluorescence quenching
Microfluidics

ABSTRACT

A warning microanalyzer for the rapid monitoring of different heavy metals in water using Carbon Dots (CDs) as selective optical reagents is presented. The synthesized CDs have different surface functionalization and exhibit selective fluorescence quenching by heavy metal ions, that combined with the use of microfluidics, provide sensitivity, ease of automation and reproducibility to the method. Moreover, they present maximum excitation wavelengths around 350 nm, allowing multiparametric analysis with a single light source. Although quantum yields range from 16 % to 78 % depending on the type of CDs, enough sensitivity is achieved for each heavy metal using the same measurement conditions of the optical detection system (lock-in modulating frequency, signal amplitude and measurement frequency). The microanalyzer is composed of a Cyclic Olefin Copolymer (COC) analytical microsystem, a flow management system, and a miniaturized customized optical detection system. In this paper, we demonstrate that our proposed system can be used as a toxicity control system by selectively measuring five different heavy metal ions (Co^{2+}, Cu^{2+}, Hg^{2+}, Ni^{2+}, and Pb^{2+}) with detection limits ranging from 2 to 12 ppb. Spiked tap water samples were analyzed, giving recoveries from 98 % to 134 %. Polluted samples containing four of the five heavy metal ions studied (Co^{2+}, Cu^{2+}, Ni^{2+}, and Pb^{2+}) were also analyzed with no significant differences observed between both methods, the proposed microanalyzer and the reference method (ICP-OES).

1. Introduction

Contamination of water by heavy metals, coming from human activities like mining or industrial wastes, has been a critical environmental concern for decades. One of the main preoccupations is their toxicity caused by the non-biodegradability and potential of bioaccumulation in different tissues and organs. The commonly employed techniques for heavy metals detection (mainly atomic absorption spectrometry (AAS) and inductively coupled plasma mass spectroscopy (ICP-MS)) require complex and expensive instrumentation and are not suitable for on-site analysis [1–5]. Currently, it is very difficult to analyze simultaneously several heavy metal ions in water with low detection limits without using these techniques and it is still a challenge to develop a sensor for on-site and real-time monitoring of various heavy metal ions with high selectivity and sensitivity [6]. There is consequently great demand for regular water quality monitoring to identify and assess heavy metal pollution in water [5].

The tendency towards on-site analysis requires new approaches and new instrumentation capable of procuring analytical information rapidly and with high sensitivity. The miniaturization of analytical procedures brings some important advantages for environmental continuous monitoring like enhanced portability and reduced reagents consumption and waste generation [7,8]. In this sense, microfluidic devices are broadly used because of the increase in surface area to volume ratio that improves process-control, reproducibility, allows the integration of different processes and yields faster reaction times [5, 9–12]. In the area of environmental pollution control and early warning systems, the combination of microelectronics and microfluidics with optical sensors is gaining importance, because of the simplicity of the integration [12,13].

Photoluminescent nanoparticles have attracted a lot of interest in recent years due to their potential applications in optical sensing [14, 15], as well as in medical and biological fields [16,17]. The use of these nanoparticles as analytical reagents enhances sensitivity, improves detection limits, and improves the stability of optical reagents [18]. Carbon Dots (CDs) show unique characteristics as optical reagents

* Corresponding author.
E-mail address: mariadelmar.puyol@uab.cat (M. Puyol).

https://doi.org/10.1016/j.snb.2022.132180
Received 15 March 2022; Received in revised form 6 May 2022; Accepted 6 June 2022
Available online 8 June 2022

because of their excellent optical properties (tuneable fluorescence emission properties, high quantum yields, and photochemical stability) [19–21] and other outstanding properties like their solubility in water, chemical inertness [22], ease of functionalization, and good biocompatibility [23]. Additionally, CDs' low toxicity highlights them as an alternative to other luminescent nanoparticles as quantum dots [24,25]. Regarding the aim of this work, N-modified CDs have also been demonstrated to provide sensitivity to heavy metals, and an easy synthesis based on cheap precursors [26,27].

In this sense, we propose an automated microanalyzer for the determination of heavy metal ions as an on-site warning system based on the fluorescence quenching effect of these ions on the emission of CDs. For the multiparametric determination and as demonstrators of heavy metal pollution, we selected five different types of CDs from the bibliography with proven selectivity to Co^{2+}, Cu^{2+}, Hg^{2+}, Ni^{2+}, and Pb^{2+}. Hydrothermal and microwave-assisted bottom-up methods [28–32] were performed to synthesize five types of CDs as reagent demonstrators of heavy metals pollution. The microanalyzer is composed of a microfluidic platform and a customized miniaturized optical detection system. The platform is fabricated in cyclic olefin copolymer (COC), which is ideal for optical detection methods because of its high transparency in near-ultraviolet and visible regions compared to other polymers [9,33] and suited to multi-layered microfabrication techniques. Signal acquisition is computer controlled and the analytical method is based on a continuous flow strategy, specifically reverse Flow Injection Analysis (rFIA). The sample is continuously flowing as a carrier, into which a specific volume of the different CDs is periodically injected [34]. In this way, a transient signal is obtained with maximum emission when the sample does not contain heavy metals, and fluorescent quenched signal when heavy metals are present in the sample [35–38]. Fluorescence (measured as the peak height) is related to the analyte concentration following the Stern-Volmer equation. Finally, FIA systems procure reproducibility and automatic baseline recovery [39].

Chemical and hydrodynamic parameters of the developed microanalyzer have been optimized to achieve the lowest limit of detection of all the heavy metals and the highest repeatability by analyzing standard solutions. Finally, its applicability has been demonstrated by measuring heavy metals in spiked tap water and extracts of polluted soil samples from areas near a lead-zinc metal smelter, increasing confidence in the accuracy and validity of the results.

2. Material and methods

2.1. Chemicals and materials

Acrylic acid, citric acid, ethylenediamine, glycerol, imidazole-2-carboxylic acid, quinine sulphate, sodium citrate, urea, the metal salts mercury (II) nitrate, nickel (II) nitrate, cobalt (II) nitrate, lead (II) nitrate, copper nitrate, zinc nitrate, cadmium nitrate, sodium nitrate, calcium nitrate, magnesium nitrate, potassium chloride and potassium carbonate were purchased from Sigma-Aldrich (Barcelona, Spain). Polyethyleneimine, branched, was purchased from Fisher Scientific (Madrid, Spain). All the CDs synthesized were purified by dialysis against MilliQ water using a Pur-A-Lyzer Mega 1000 dialysis kit with a cut-off of 1 kDa.

Dispersions for the CDs syntheses and citric/citrate buffer were prepared in MilliQ water. All solutions for the microanalyzer characterization and the metal ion sensing were buffered at pH 4 with a 0.1 M citric/citrate buffer.

Cyclic Olefin Copolymer (COC) sheets were supplied from TOPAS Advanced Polymers GmbH (Florence, KY, USA).

2.2. Apparatus

A Labolan IDL.AI36 oven (Navarra, Spain) was used for the hydrothermal synthesis processes and a Bifinett KH 1106 domestic microwave oven for the microwave-assisted processes.

Absorption spectra were acquired with a Shimadzu UV-3101PC UV-Vis-NIR double beam spectrophotometer (Kyoto, Japan) and fluorescence spectra were registered with a Horiba Jobin Yvon Fluorolog FL3–11 spectrofluorometer (Longjumeau, France). Dynamic Light Scattering (DLS) measurements were performed in a Microtrac Nanotrac Flex nanoparticle size analyzer (Krefeld, Germany). High-Resolution Transmission Electron Microscopy (HR-TEM) images were taken on a high-resolution JEOL JEM-2011 Microscope (Tokyo, Japan).

2.3. Microfluidic platform and experimental setup

The fabrication process of the microfluidic platform starts with the design of the different layers with Computer-Aided Design (CAD) software. Every COC layer substrate was machined on an LPKF Laser and Electronics Protomat S63 Computer Numerical Control (CNC) micromilling machine (Garbsen, Germany). The different layers were thermolaminated using a Talleres Francisco Camps hydraulic press (Granollers, Spain). The microfluidic platform is formed by a structural layer of TOPAS 5013, which was previously laminated with two films of lower glass transition temperature (TOPAS 8007) acting as sealing layers [40], and two outer layers of TOPAS 5013. Once overlapped and aligned, COC tapes were laminated to obtain the final device. As it can be seen in Fig. 1A, the microfluidic platform (30 mm wide, 50 mm height, and 2 mm depth) has two inlets, a two-dimensional meander micromixer (0.8 mm wide and 1 mm depth), an optical flow cell (4.5 mm diameter and 1 mm depth), and an outlet.

The experimental setup is based on a rFIA, where CDs are sequentially injected into a blank (buffer solution) and samples (standard solutions, spiked tap water and soil extracts). The microfluidic set-up allows the pre-buffering of the samples by an in-line T connector mixer (sample/buffer solution in 1:1 proportion). For continuous flow injection, the microfluidic platform was connected with 0.8 mm internal diameter Teflon tubing (Tecnyfluor, Barcelona, Spain), to a Gilson Minipuls 2 peristaltic pump (Middleton, WI, USA) fitted with 1.14 mm internal diameter Tygon tubing (Ismatec, Wertheim, Germany). Connections were secured with O-rings FPM75 (Epidor, Barcelona, Spain). A Hamilton MVP TMI-6116 six-port injection valve (Bonaduz, Switzerland) was used to inject the CDs.

The microfluidic platform is inserted in a customized miniaturized optical detection system (Fig. 1B) by using an Optical Lock and Key Reader approach [8]. It consists of a LED emitting at 365 nm (OSA Opto Light GmbH EOLD-365–525), a Thorlabs 460/60 25 mm band-pass filter (Munich, Germany), and a PIN photodetector (Hamamatsu S1337–66BR) with 33 mm^2 of active area mounted and integrated on a printed circuit board (PCB). The optical detection system is modulated

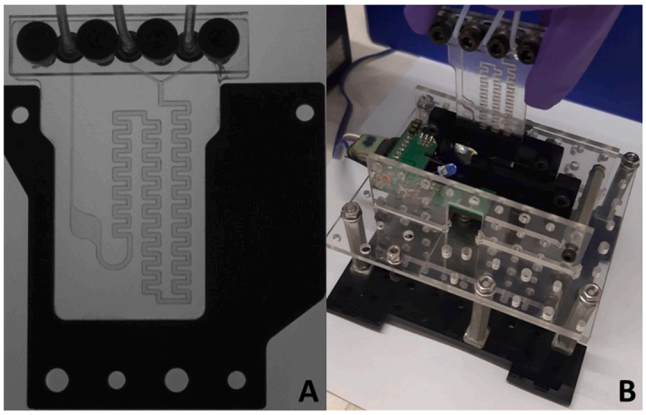

Fig. 1. (A) Microfluidic platform fabricated for the heavy metal ions detection. (B) Customized miniaturized optical detection system with the microfluidic platform inserted.

with a digital lock-in amplifier to avoid light interferences and the signal is obtained with a NI USB-6211 Data Acquisition Card (National Instruments, Austin, TX, USA).

2.4. CDs synthesis and optical characterization

Five different CDs were synthesized following published synthesis procedures: CDs synthesized with citric acid and ethylenediamine (ED CDs) [28], CDs synthesized with citric acid and polyethyleneimine (PEI CDs) [29], CDs synthesized with glycerol and ethylenediamine (EA CDs) [30], CDs synthesized with citric acid, urea, and imidazole (UREA CDs) [31], CDs synthesized with acrylic acid and ethylenediamine (ACR CDs) [32]. All batches were dialyzed against MilliQ water using a dialysis membrane with a cut-off of 1 kDa for their purification and kept in a refrigerator. Since the concentration of the CDs is unknown, dilution factors in citric/citrate buffer are used as an approximate measurement.

Absorption spectra and photoluminescence spectra (excitation and emission) of CDs' water dispersions were obtained. Quantum Yields (QYs) were calculated with the optically dilute measurement method [41] using quinine sulphate in 0.1 M sulphuric acid as a standard.

2.5. Optimization of the chemical and hydrodynamic parameters of the microanalyzer

Some chemical and hydrodynamic parameters were optimized using a univariate optimization procedure taking as compromise signal to noise ratio and sensitivity for all the five target heavy metals.

Citric/citrate buffer solutions prepared at four different pH values (3, 4, 5, and 6) and four different concentration levels (0.001, 0.01, 0.1 and 1 M) were tested to obtain the maximum fluorescence signal and taking into account the solubility of the different heavy metal ions.

Regarding hydrodynamic parameters, the flow rate of the sample (carrier) was tested from 0.5 to 2 mL/min and CDs injection volume from 0.1 to 1 mL. Moreover, some operational parameters of the optical detection system like signal amplification and integration time were optimized. In this case, CDs were injected into buffer solution and 0.01 ppm heavy metal standard solutions to evaluate the signal to noise ratio and detection limit.

Finally, different dilution factors of the CDs dispersions were also tested. For the five types of CDs, 10, 50, 100, 500 and 1000 dilutions in buffer solution, were prepared.

2.6. Characterization of CDs selectivity

Before performing photoluminescence studies of the synthesized CDs, a dilution was done to obtain an absorption of 0.05 a.u. and avoid possible self-absorption effects.

Selectivity of the different CDs was firstly tested in batch against different heavy metal ion solutions (Cd^{2+}, Co^{2+}, Cu^{2+}, Hg^{2+}, Ni^{2+}, Pb^{2+}, Zn^{2+}), and other potentially interfering ions present in water (Na^{+}, Mg^{2+}, Ca^{2+}, Cl^{-}, CO_3^{2-}). Emission spectra of 0.5 mL of the corresponding CD dispersion at the optimized dilution factor showing an absorption of 0.05 a.u. with the addition of 2.5 mL of citric/citrate buffer at pH 4 were compared with the same CDs dispersion with the addition of 2.5 mL of a buffered solution containing a specific ion at a concentration of 10 ppm (in the case of the heavy metal ions) or at a concentration of 1000 ppm (for other potentially interfering ions) after the dilution in the cuvette.

2.7. Analytical quality parameters of the microanalyzer

Selectivity was tested in the microfluidic system using several standard solutions with a 0.5 ppm concentration of the target heavy metal (Co^{2+}, Cu^{2+}, Hg^{2+}, Ni^{2+}, and Pb^{2+} in each case). Every standard solution also contained the rest of the heavy metal ions tested at a concentration of 10 ppm and the other potentially interfering ions tested at a concentration of 1000 ppm.

Limit of detection was evaluated from the calibration curves obtained by injecting per triplicate each type of CDs in standard solutions containing increasing concentrations of the five heavy metals studied (0.01, 0.05, 0.1, 0.5, and 1 ppm) and the other interfering ions. Fluorescence quenching of the CDs was studied through the Stern-Volmer equation [42].

Repeatability of the analytical system was evaluated by performing ten injections of each CD into a standard solution containing 0.5 ppm of each target heavy metal and the other studied ions.

2.8. Samples analysis

To assess the applicability of this method, spiked tap water samples and extracts of polluted soil samples were tested. Tap water samples were spiked to obtain concentrations of 0.03, 0.06, 0.1, 0.4, and 0.8 ppm of the target heavy metals. They were also spiked with the rest of the heavy metal ions tested at a concentration of 10 ppm and the other potentially interfering ions tested at a concentration of 1000 ppm.

Nitric acid extracts of polluted soil samples coming from the neighbourhood of a smelter plant (located in Torreon, Mexico) and containing high concentrations of four of the five heavy metals studied (Hg^{2+} is not present), were directly supplied, and analyzed by the reference method ICP-OES and the proposed microanalyzer, for comparison purposes. 0.5 g of the samples were digested with 10 mL of nitric acid in a Milestone Ultrawave microwave digestion system at 175ºC for 15 min. Samples were filtered with a 0.45 μm filter, diluted to 50 mL with MilliQ water, and finally analyzed with a Perkin-Elmer Optima 4300DV spectrometer.

Calibration curves were performed with standard solutions at higher concentrations (different concentration ranges depending on the analyte). As stated, to avoid pH changes of these acid extracts, samples were automatically buffered in the system before the injection of the CDs. Moreover, an exhaustive cleaning of the microsystem consisting of flowing buffer solution for 2 min was necessary between samples.

3. Results and discussion

3.1. CDs characterization

As reproducibility and characteristics of the synthesized CDs will impact directly on the analytical results and reproducibility of the analytical method, CDs were fully characterized. Regarding optical properties, they show similar absorbance and photoluminescence spectra, with a wide absorption band around 350 nm and a wide emission band around 450 nm, obtaining Stokes' shifts of approximately 100 nm in all cases, as it can be seen in Fig. 2. Therefore, all of them could be used as optical reagents with the same miniaturized optical set-up.

QYs were calculated, obtaining values of 78 % for ED CDs, 32 % for PEI CDs, 16 % for EA CDs, 44 % for UREA CDs, and 25 % for ACR CDs.

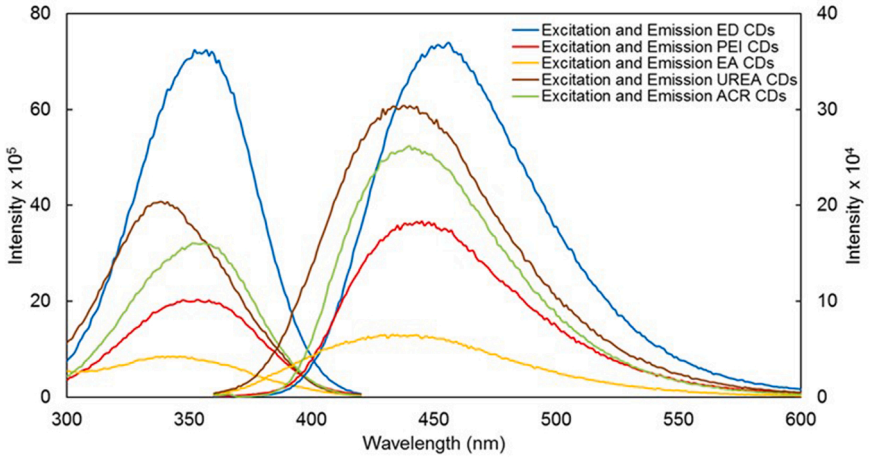

Fig. 2. : Excitation and emission spectra of the five synthesized CDs.

Size and shape were obtained with HR-TEM images and DLS measurements. Results showed spherical shape nanoparticles with sizes ranging from 2 to 4 nm. Although high-quality contrast images are difficult to obtain with CDs with HR-TEM, we observed two populations of CDs, one with a crystalline structure, where the diffraction planes could be distinguished and the other amorphous one.

3.2. CDs selectivity tests in batch

First, the quenching effect of different heavy metals, and other potentially interfering ions present in water was investigated in batch. A great number of publications demonstrate that different types of N-modified CDs present very strong interactions towards different heavy metal ions through the surface functional groups (-COOH, -OH, -CONH-) [28–32]. According to the bibliography and as shown in the supplementary information (Fig. S2A-E), each CD dispersion was selective to a specific heavy metal. ED CDs show good selectivity to Hg^{2+}, PEI CDs to Cu^{2+}, EA CDs to Pb^{2+}, UREA CDs to Ni^{2+}, and ACR CDs to Co^{2+}. The quenching effect of all the other tested ions was not significant. In these experiments, it could also be noticed the different sensitivity of the synthesized CDs to the target heavy metal, which would affect the optimization of the measurement conditions of the optical detection system of the microanalyzer for multiparametric measurements.

3.3. Optimization of the microanalyzer

Different chemical, hydrodynamic and optical measuring variables of the microanalyzer were optimized to make possible the multiparametric detection of heavy metals in water, as a compromise between the best S/N, limits of detection, response time and reagents saving. Tested values intervals and the final optimal selected values are shown in Table 1.

Table 1
Optimization of chemical, operational and hydrodynamic parameters.

Parameter	Tested interval	Optimal value
Buffer concentration (M)	0.001 – 1.000	0.100
Buffer pH	3 – 6	4
Injection volume (mL)	0.1 – 1.0	0.5
Carrier flow rate (mL/min)	0.5 – 2.0	1.5
Signal amplification	1 – 100	10
Integration time (s)	0.1 – 1.0	0.1
ED CDs dilution factor	10–1000	100
PEI CDs dilution factor	10–1000	50
EA CDs dilution factor	10–1000	10
UREA CDs dilution factor	10–1000	50
ACR CDs dilution factor	10–1000	10

As an example, Fig. 3A shows optimization of the buffer pH. The optical properties of CDs are sensitive to pH due to the ionizable functional groups on the surface. Therefore, the analytical system must operate at a constant pH. In general, the higher the pH, the higher the fluorescence of the CDs. However, the selected pH must ensure to have heavy metal species free in solution. As it can be seen, the highest fluorescence intensity is obtained at pH 4 for all the different CDs. On the other hand, the effect of the flow rate on the measured signal can be seen in Fig. 3B with the injection of 0.5 mL of a dilution of 100 of ED CDs into a 0.1 M citric/citrate buffer at pH 4 as an example. A faster flow rate implies a more rapid analysis and therefore, higher sample throughput, which are desirable. However, slightly less intense peaks are obtained because the sample is less time in contact with the CDs. The lower is the flow rate, the wider and more intense are the obtained peaks until achieving the steady-state signal. Therefore, a 1.5 mL/min sample flow rate was chosen as the optimal one for subsequent experiments. At this flow rate, response time is calculated in 50 s

3.4. Analytical quality parameters of the microanalyzer

Analytical quality parameters were calculated from calibration curves obtained performing the separate analysis of each heavy metal at the optimized operational values. Fig. 4A show the transient response of the microsystem by injecting the five optimized CDs dispersions into buffer solution and into 0.5 ppm standard solutions of the target heavy metal (Co^{2+}, Cu^{2+}, Hg^{2+}, Ni^{2+}, and Pb^{2+}) which also contained the rest of the heavy metal ions tested at a concentration of 10 ppm and the other potentially interfering ions tested at a concentration of 1000 ppm. Results obtained confirm the selectivity of the different CDs tested in batch. The fluorescence signal quickly returned to the baseline after each signal peak and there was not any significant signal drift of the baseline. This demonstrates the robustness of the microanalyzer for the proposed application.

Calibration curves showed a good linear correlation between 0.01 and 1 ppm, as can be seen in Fig. 4B. And even though the Stern-Volmer model has some limitations that affect the accuracy, caused by deviations at high concentrations [43,44], concentration ranges as high as 50–600 ppm were tested for real polluted samples, showing also good linear correlation but lower sensitivity.

Detection limits, LODs (Table 2) were calculated as 3 SD/K_{SV} (where SD is the standard deviation of the blank and K_{SV} (Stern-Volmer constant) is the slope of the linear fit near to unity).

Repeatability was calculated as relative standard deviation (RSD) obtained with 10 repeated injections of the same CDs into the 0.5 ppm heavy metal standard solutions. Data is detailed in Table 2, showing values under 1.2%.

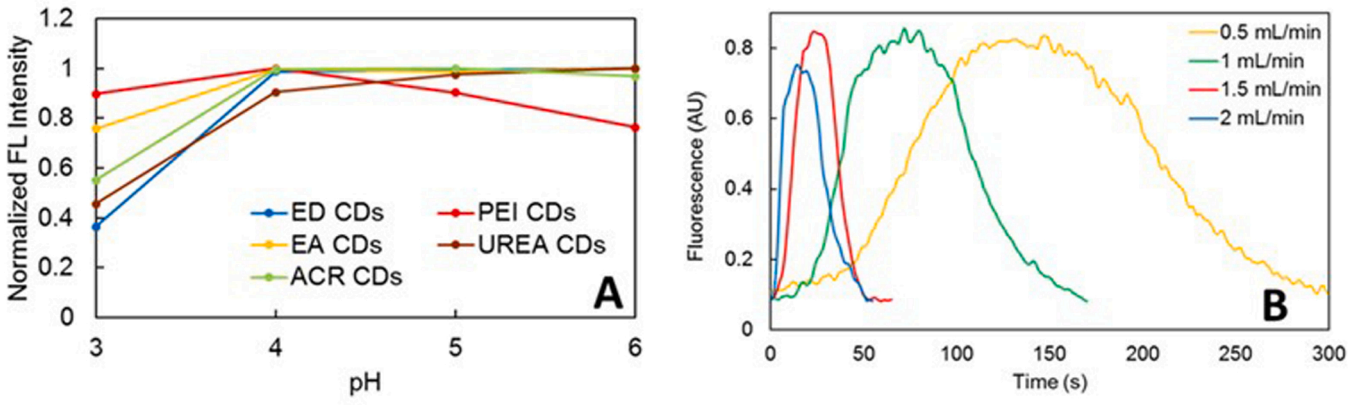

Fig. 3. (A) Normalized fluorescence intensity obtained by injecting the five CDs at their optimal dilution factor into 0.1 M citric/citrate buffer solutions of different pH values. (B) Effect of flow rate into the obtained signal for an injection of 0.5 mL of ED CDs (100 dilution factor) into buffer solution.

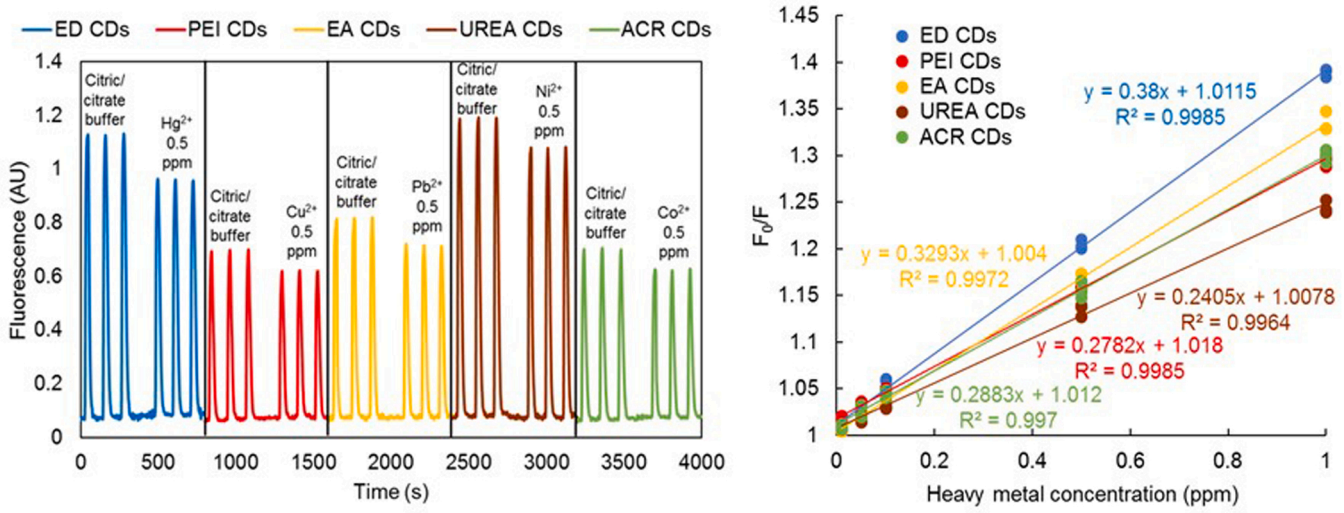

Fig. 4. (A) Transient response of the microsystem by injecting the CDs into buffer solution (as intensity value with no quencher) and to different standard solutions of heavy metals containing potential interferents (Zn^{2+}, Cd^{2+}, Na^{+}, Mg^{2+}, Ca^{2+}, Cl^{-}, CO_3^{2-}). (B) Stern-Volmer representation of quenching effect of the target heavy metals on the fluorescence of the five types of CDs.

Table 2
Results summarizing the analytical performance of the proposed microanalyzer for the monitoring of heavy metals in water samples.

Type of CDs	Selectivity	K_{SV} (ppm^{-1})	Detection Limit (ppb)	RSD (%)
ED CDs	Hg^{2+}	0.3800	5.9 ± 0.8	0.5
PEI CDs	Cu^{2+}	0.2782	11.7 ± 0.7	1.2
EA CDs	Pb^{2+}	0.3293	8.8 ± 0.8	1.1
UREA CDs	Ni^{2+}	0.2405	2.5 ± 0.3	0.4
ACR CDs	Co^{2+}	0.2883	3.9 ± 0.5	0.9

3.5. Samples analysis

Spiked tap water samples were analyzed at the optimized conditions and after performing a calibration experiment for each heavy metal. Table 3 shows recovery rates. In general, an overestimation is noticed for the less concentrated samples near the limit of detection. At this concentration level, results are also less precise because the error of the interpolated signal is higher at lower concentrations. However, as a warning system, results allow determining the estimated value of heavy metals as indicators of pollution.

To validate the usability of the developed microanalyzer, real polluted soil samples taken from areas surrounding a metallurgic industry were analyzed. Nitric acid extracts were prepared and analyzed by a reference method (ICP-OES) and the proposed microanalyzer. Fig. 5 shows, as an example, the calibration curve for Co^{2+} at a higher concentration range (10–70 ppm) where it can be noticed from the slope of the calibration curve a lower sensitivity. Fig. 6 shows the comparative test for the measurement of Co^{2+} in 8 different samples. Regression equations of the comparison test (intercept, slope, and correlation coefficient) for the five heavy metal ions as well as t_{calc} values obtained with the paired t-test are shown in the Supplementary Information (Table S1). From the statistical data treatment, it can be concluded results obtained with the developed microanalyzer were not significantly different from the ones measured with the reference method according to the paired t-test ($t_{calc} < t_{tab}$) for the four heavy metals analyzed.

Table 4 shows accuracy expressed as % error for the differences between results obtained with both methods. As it can be seen, accuracy is different for each heavy metal and, as it is more affected at lower concentrations, the determination of Pb^{2+} is less accurate. However, a maximum value of 7.5% error is calculated.

4. Conclusions

In this paper we have developed a new multiparametric microanalyzer as a warning system for heavy metals pollution monitoring.

Table 3
Determination of the heavy metals studied in spiked tap water samples.

Sample	Concentration of the analyte in the sample (ppm)	Analyte recovery rates				
		Hg^{2+}	Cu^{2+}	Pb^{2+}	Ni^{2+}	Co^{2+}
Spiked tap water	0.03	129 %	131 %	134 %	123 %	120 %
	0.06	116 %	112 %	120 %	110 %	111 %
	0.1	105 %	103 %	105 %	104 %	105 %
	0.4	101 %	100 %	102 %	100 %	100 %
	0.8	99.1 %	99.0 %	101 %	98.8 %	98.2 %

Thanks to the reduced dimensions of the fluidic system, it consumes small volumes of reagents and has a fast analysis time. Although sample treatment (buffering) must be performed, which for acid extracts was crucial, this is performed by the same flow management systems before CDs are injected. Performance of the microanalyzer, tested with standard solutions, spiked tap water and real samples, combined with the stability of the luminescent reagents (N-modified CDs) demonstrates its potential application for long-term and continuous monitoring of heavy metals in water. Five different heavy metals (Co^{2+}, Cu^{2+}, Hg^{2+}, Ni^{2+} and Pb^{2+}) have been selectively detected. However, it is possible to expand the analytes to determine, as far as other selective CDs (with absorption bands around 350 nm) could be synthesized. In most of the cases, LODs comply with the regulation [5] concerning heavy metal pollution in water (between 2 and 12 ppb) but in the case of Hg^{2+}, the established LOD is still lower. Some future work must be conducted in order to finally validate the real applicability of the proposed methodology for heavy metals monitoring, such as long-term studies. Despite current maintenance criteria of quality control stations is approximately every 15 days and no critical issues are expected regarding the stability of CDs, this should be assessed. Taking into account results for repeatability, selectivity, recoveries of spiked tap water samples and accuracy of real polluted samples, we demonstrate its applicability as an on-site warning system of heavy metals contamination.

Although the presented set-up requires bulky components for flow management in continuous mode, such as a peristaltic pump, the equipment can be further miniaturized, and it is easily automatable. We are currently working on the development of an automatic and computer-controlled microanalyzer based on the use of solenoid peristaltic micro-pumps and three-way solenoid valves, enabling automation of the whole analytical procedure.

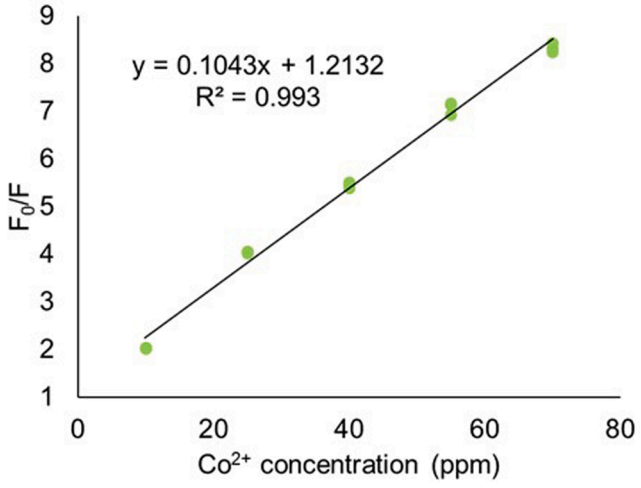

Fig. 5. : Stern-Volmer representation of quenching effect of Co^{2+} on the fluorescence of ACR CDs in a higher concentration range (10–70 ppm).

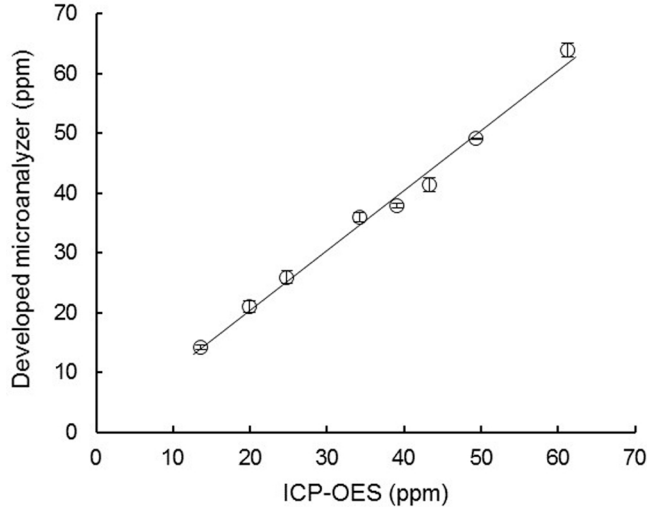

Fig. 6. : Comparative study between the results for the analysis of Co^{2+} in polluted soil samples (n = 8) obtained by the developed microanalyzer and the reference method (ICP-OES).

CRediT authorship contribution statement

Alex Pascual-Esco: Methodology Development, Investigation, Data analysis, Statistical analysis, Validation and Writing – original draft. **Julián Alonso-Chamarro:** Resources, Project administration, Funding acquisition, and Writing – review & editing. Mar Puyol: Research Conceptualization, Resources, Supervision, Project administration,

Table 4
Concentration of the heavy metals studied in polluted soil samples determined by the reference method (ICP-OES) and with the proposed method, and accuracy expressed as (% error).

Sample number	$[Cu^{2+}]$ ICP-OES (ppm)	$[Cu^{2+}]$ proposed method (ppm)	% error	$[Pb^{2+}]$ ICP-OES (ppm)	$[Pb^{2+}]$ proposed method (ppm)	% error
1	576.2	587.0	1.9	11.5	12.0	4.8
2	255.7	251.1	1.8	4.8	4.9	2.1
3	511.7	507.3	0.9	5.3	5.2	1.7
4	119.7	116.2	2.9	3.7	3.9	7.4
5	231.9	236.5	2.0	4.0	4.0	1.0
6	458.3	477.9	4.3	7.1	7.0	1.3
7	90.5	92.2	1.9	0.8	0.8	4.0
8	95.7	92.4	3.4	2.2	2.3	7.5
Sample number	**$[Ni^{2+}]$ ICP-OES (ppm)**	**$[Ni^{2+}]$ proposed method (ppm)**	**% error**	**$[Co^{2+}]$ ICP-OES (ppm)**	**$[Co^{2+}]$ proposed method (ppm)**	**% error**
1	42.3	42.8	1.0	49.4	49.1	0.5
2	31.8	31.6	0.7	34.2	36.0	5.1
3	61.3	61.9	1.0	61.3	63.9	4.3
4	35.8	35.9	0.3	24.8	26.0	4.8
5	57.9	58.7	1.4	39.1	37.9	3.1
6	33.4	32.9	1.4	43.3	41.4	4.4
7	25.7	26.4	3.1	13.6	14.3	4.5
8	33.9	35.4	4.4	19.9	21.0	5.7

Funding acquisition, and Writing – original draft.

Declaration of Competing Interest

The authors declare that they have no known competing financial interests or personal relationships that could have appeared to influence the work reported in this paper.

Acknowledgements

We gratefully thank the Instituto Tecnológico de la Laguna (Torreón, México) for soil samples supply and Dr. Eva Arasa for the soil extracts preparation. This work has been financially supported by the Spanish Ministry of Science and Innovation (MICINN) through project CTQ2017-85011-R and project PID2020-117216RB-I00, co-funded by FEDER (Fondo Europeo de Desarrollo Regional), and the Catalonia Government through 2017SGR-220. The support of Met-Mex Peñoles for the development of this work was also gratefully acknowledged.

Appendix A. Supporting information

Supplementary data associated with this article can be found in the online version at doi:10.1016/j.snb.2022.132180.

References

[1] Z. Wang, C. Xu, Y. Lu, X. Chen, H. Yuan, G. Wei, G. Ye, J. Chen, Fluorescence sensor array based on amino acid derived carbon dots for pattern-based detection of toxic metal ions, Sens. Actuators B Chem. 241 (2017) 1324–1330, https://doi.org/10.1016/j.snb.2016.09.186.

[2] C.Y. Wang, C.C. Hsu, Online, continuous, and interference-free monitoring of trace heavy metals in water using plasma spectroscopy driven by actively modulated pulsed power, Environ. Sci. Technol. 53 (2019) 10888–10896, https://doi.org/10.1021/acs.est.9b02970.

[3] N. Ullah, M. Mansha, I. Khan, A. Qurashi, Nanomaterial-based optical chemical sensors for the detection of heavy metals in water: recent advances and challenges, Trends Anal. Chem. 100 (2018) 155–166, https://doi.org/10.1016/j.trac.2018.01.002.

[4] J.P. Devadhasan, J. Kim, A chemically functionalized paper-based microfluidic platform for multiplex heavy metal detection, Sens. Actuators B Chem. 273 (2018) 18–24, https://doi.org/10.1016/j.snb.2018.06.005.

[5] A. Lace, J. Cleary, A review of microfluidic detection strategies for heavy metals in water, Chemosensors 9 (60) (2021) 1–26, https://doi.org/10.3390/chemosensors9040060.

[6] X. Liu, Y. Wang, Y. Song, Visually multiplexed quantitation of heavy metal ions in water using volumetric bar-chart chip, Biosens. Bioelectron. 117 (2018) 644–650, https://doi.org/10.1016/j.bios.2018.06.046.

[7] Ö. Biçen Ünlüer, F. Ghorbani-Bidkorbeh, R. Keçili, C. Mustansar Hussain, Future of the modern age of analytical chemistry: Nanominiaturization, in: C. Mustansar Hussain (Ed.), Handbook on Miniaturization in Analytical Chemistry: Application of Nanotechnology, Elsevier, Amsterdam, 2020, pp. 277–296.

[8] O. Ymbern, M. Berenguel-Alonso, A. Calvo-López, S. Gómez-de Pedro, D. Izquierdo, J. Alonso-Chamarro, Versatile lock and key assembly for optical measurements with microfluidic platforms and cartridges, Anal. Chem. 87 (2015) 1503–1508, https://doi.org/10.1021/ac504255t.

[9] R.K. Jena, C.Y. Yue, Y.C. Lam, Micro fabrication of cyclic olefin copolymer (COC) based microfluidic devices, Microsyst. Technol. 18 (2012) 159–166, https://doi.org/10.1007/s00542-011-1366-z.

[10] N. Yogarajaha, S.S.H. Tsai, Detection of trace arsenic in drinking water: challenges and opportunities for microfluidics, Environ. Sci.: Water Res. Technol. 1 (2015) 426–447, https://doi.org/10.1039/c5ew00099h.

[11] L. Lin, Y. Yin, S.A. Starostin, H. Xu, C. Li, K. Wu, C. He, V. Hessel, Microfluidic fabrication of fluorescent nanomaterials: a review, Chem. Eng. J. 425 (131511) (2021) 1–15, https://doi.org/10.1016/j.cej.2021.131511.

[12] H. Gai, Y. Li, E.S. Yeung, Optical detection systems on microfluidic chips, in: B. Lin (Ed.), Microfluidics: Technologies and Applications, Springer, Berlin, 2011, pp. 171–201.

[13] K.A. Lukyanenko, I.A. Denisov, V.V. Sorokin, A.S. Yakimov, E.N. Esimbekova, P. I. Belobrov, Handheld enzymatic luminescent biosensor for rapid detection of heavy metals in water samples, Chemosensors 7 (2019) 1–10, https://doi.org/10.3390/chemosensors7010016.

[14] M. Berenguel-Alonso, I. Ortiz-Gómez, B. Fernández, P. Couceiro, J. Alonso-Chamarro, L.F. Capitán-Vallvey, A. Salinas-Castillo, M. Puyol, An LTCC monolithic microreactor for the synthesis of carbon dots with photoluminescence imaging of the reaction progress, Sens. Actuators B Chem. 296 (126613) (2019) 1–8, https://doi.org/10.1016/j.snb.2019.05.090.

[15] F. Copur, N. Bekar, E. Zor, S. Alpaydin, H. Bingol, Nanopaper-based photoluminescent enantioselective sensing of L-Lysine by L-Cysteine modified carbon quantum dots, Sens. Actuators B Chem. 279 (2019) 305–312, https://doi.org/10.1016/j.snb.2018.10.026.

[16] M.L.C. Passos, P.C.A.G. Pinto, J.L.M. Santos, M.L.M.F.S. Saraiva, A.R.T.S. Araujo, Nanoparticle-based assays in automated flow systems: a review, Anal. Chim. Acta 889 (2015) 22–34, https://doi.org/10.1016/j.aca.2015.05.052.

[17] Y. Liu, F. Seidi, C. Deng, R. Li, T. Xu, H. Xiao, Porphyrin derived dual-emissive carbon quantum dots: customizable synthesis and application for intracellular Cu2 + quantification, Sensors Actuators B Chem. 343 (2021), 130072, https://doi.org/10.1016/j.snb.2021.130072.

[18] T. Chen, S. Yin, J. Wu, Nanomaterials meet microfluidics: improved analytical methods and high-throughput synthetic approaches, Trends Anal. Chem. 142 (116309) (2021) 1–19, https://doi.org/10.1016/j.trac.2021.116309.

[19] K.J. Mintz, Y. Zhou, R.M. Leblanc, Recent development of carbon quantum dots regarding their optical properties, photoluminescence mechanism, and core structure, Nanoscale 11 (2019) 4634–4652, https://doi.org/10.1039/c8nr10059d.

[20] A. Simpson, R.R. Pandey, C.C. Chusuei, K. Ghosh, R. Patel, A.K. Wanekaya, Fabrication characterization and potential applications of carbon nanoparticles in the detection of heavy metal ions in aqueous media, Carbon 127 (2018) 122–130, https://doi.org/10.1016/j.carbon.2017.10.086.

[21] R. Jelinek, Carbon Quantum Dots: Synthesis, Properties and Applications, electronic ed, Springer, Cham (Switzerland), 2017.

[22] Y. Wang, A. Hu, Carbon quantum dots: synthesis, properties and applications, J. Mater. Chem. C. 2 (2014) 6921–6939, https://doi.org/10.1039/c4tc00988f.

[23] S. Anwar, H. Ding, M. Xu, X. Hu, Z. Li, J. Wang, L. Liu, L. Jiang, D. Wang, C. Dong, M. Yan, Q. Wang, H. Bi, Recent advances in synthesis, optical properties, and biomedical applications of carbon dots, ACS Appl. Bio Mater. 2 (6) (2019) 2317–2338, https://doi.org/10.1021/acsabm.9b00112.

[24] M.L. Liu, B.B. Chen, C.M. Li, C.Z. Huang, Carbon dots: synthesis, formation mechanism, fluorescence origin and sensing applications, Green. Chem. 21 (2019) 449–471, https://doi.org/10.1039/c8gc02736f.

[25] J.H. Liu, Y. Wang, G.H. Yan, F. Yang, H. Gao, Y. Huang, H. Wang, P. Wang, L. Yang, Y. Tang, L.R. Teisl, Y.P. Sun, Systematic toxicity evaluations of high-performance carbon "Quantum" dots, J. Nanosci. Nanotechnol. 19 (4) (2019) 2130–2137, https://doi.org/10.1166/jnn.2019.15807.

[26] X. Sun, Y. Lei, Fluorescent carbon dots and their sensing applications, Trends Anal. Chem. 89 (2017) 163–180, https://doi.org/10.1016/j.trac.2017.02.001.

[27] P. Li, S.F.Y. Li, Recent advances in fluorescence probes based on carbon dots for sensing and speciation of heavy metals, Nanophotonics 10 (2) (2020) 877–908, https://doi.org/10.1515/nanoph-2020-0507.

[28] F. Du, F. Zeng, Y. Ming, S. Wu, Carbon dots-based fluorescent probes for sensitive and selective detection of iodide, Microchim. Acta 180 (2013) 453–460, https://doi.org/10.1007/s00604-013-0954-2.

[29] A. Salinas-Castillo, M. Ariza-Avidad, C. Pritz, M. Camprubí-Robles, B. Fernández, M.J. Ruedas-Rama, A. Megia-Fernández, A. Lapresta-Fernández, F. Santoyo-Gonzalez, A. Schrott-Fischer, L.F. Capitan-Vallvey, Carbon dots for copper detection with down and upconversion fluorescent properties as excitation sources, Chem. Commun. 49 (2013) 1103–1105, https://doi.org/10.1039/c2cc36450f.

[30] Y. Jiang, Y. Wang, F. Meng, B. Wang, Y. Cheng, C. Zhu, N-doped carbon dots synthesized by rapid microwave irradiation as highly fluorescent probes for Pb2+ detection, N. J. Chem. 39 (2015) 3357–3360, https://doi.org/10.1039/c5nj00170f.

[31] X. Wang, D. Wang, Y. Guo, C. Yang, A. Iqbal, W. Liu, W. Qin, D. Yan, H. Guo, Imidazole derivative-functionalized carbon dots: using as a fluorescent probe for detecting water and imaging of live cells, Dalton Trans. 44 (2015) 5547–5554, https://doi.org/10.1039/c5dt00128e.

[32] N. Jing, M. Tian, Y. Wang, Y. Zhang, Nitrogen-doped carbon dots synthesized from acrylic acid and ethylenediamine for simple and selective determination of cobalt ions in aqueous media, J. Lumin. 206 (2019) 169–175, https://doi.org/10.1016/j.jlumin.2018.10.059.

[33] M. Denz, G. Brehm, C.Y.J. Hémonnot, H. Spears, A. Wittmeier, C. Cassini, O. Saldanha, E. Perego, A. Diaz, M. Burghammerd, S. Köster, Cyclic olefin copolymer as an X-ray compatible material for microfluidic devices, Lab Chip 18 (2018) 171–178, https://doi.org/10.1039/c7lc00824d.

[34] L. Chen, J. Xu, T. Wang, Y. Huang, D. Yuan, Z. Gong, Toward a versatile flow technique: Development and application of reverse flow dual-injection analysis (rFDIA) for determining dissolved iron redox species and soluble reactive phosphorus in seawater, Talanta 232 (122404) (2021) 1–9, https://doi.org/10.1016/j.talanta.2021.122404.

[35] C. Hu, T.J. Lin, Y.C. Huang, Y.Y. Chen, K.H. Wang, K.Y.A. Lin, Photoluminescence quenching of thermally treated waste-derived carbon dots for selective metal ion sensing, Environ. Res. 197 (111008) (2021) 1–10, https://doi.org/10.1016/j.envres.2021.111008.

[36] F. Zu, F. Yan, Z. Bai, J. Xu, Y. Wang, Y. Huang, X. Zhou, The quenching of the fluorescence of carbon dots: a review on mechanisms and applications, Microchim. Acta 184 (2017) 1899–1914, https://doi.org/10.1007/s00604-017-2318-9.

[37] H. Lee, Y.C. Su, H.H. Tang, Y.S. Lee, J.Y. Lee, C.C. Hu, T.C. Chiu, One-Pot hydrothermal synthesis of carbon dots as fluorescent probes for the determination of mercuric and hypochlorite ions, Nanomaterials 11 (1831) (2021) 1–11, https://doi.org/10.3390/nano11071831.

[38] C. Zhang, S. Wu, Y. Yu, F. Chen, Determination of thiourea based on the reversion of fluorescence quenching of nitrogen doped carbon dots by Hg2+, Spectrochim, Acta A 227 (117666) (2020) 1–6, https://doi.org/10.1016/j.saa.2019.117666.

[39] S. Karada, E.M. Görüsük, E. Çetinkaya, S. Deveci, K.B. Dönmez, E. Uncuoglu, M. Dogu, Development of an automated flow injection analysis system for determination of phosphate in nutrient solutions, J. Sci. Food Agric. 98 (2018) 3926–3934, https://doi.org/10.1002/jsfa.8911.

[40] TOPAS Advanced Polymers. http://www.topas.com, 2021 (Accessed October 28, 2021).
[41] G.A. Crosby, J.N. Demas, The measurement of photoluminescence quantum yields. A review, J. Phys. Chem. 75 (1971) 991–1024, https://doi.org/10.1021/j100678a001.
[42] Y. Song, S. Zhu, S. Xiang, X. Zhao, J. Zhang, H. Zhang, Y. Fu, B. Yang, Investigation into the fluorescence quenching behaviours and applications of carbon dots, Nanoscale 6 (2014) 4676–4682, https://doi.org/10.1039/c4nr00029c.
[43] A. de la Torre, S. Medina-Rodríguez, J.C. Segura, J.F. Fernández-Sánchez, A polynomial-exponent model for calibrating the frequency response of photoluminescence-based sensors, Sensors 20 (2020) 4635, https://doi.org/10.3390/s20164635.
[44] T. Htun, A negative deviation from stern–volmer equation in fluorescence quenching, J. Fluoresc. 14 (2004) 217–222, https://doi.org/10.1023/B:JOFL.0000016294.96775.fd.

Alex Pascual-Esco received a degree in Chemistry from Universitat Autònoma de Barcelona (UAB) in 2017. In 2018 obtained a Master's degree in Analytical Chemistry form Universitat de Barcelona (UB). Since October 2018, he is a Ph.D. candidate at the Sensors and Biosensors Group under the supervision of Dr. Mar Puyol. His research interests include the design and fabrication of microsystems for water quality monitoring (μTAS) based on LTCC and polymer technologies, microfluidic platforms for the synthesis of nanomaterials and optical sensors.

Julián Alonso-Chamarro received his Ph.D. in Analytical Chemistry in 1987 at the Autonomous University of Barcelona. He is Professor of Analytical Chemistry at the same university. He has co-authored more than 140 research papers on (Bio)chemical sensors and automated flow systems and is author of different patents about sensors and analytical instrumentation for environmental monitoring. His research interests include the design and fabrication of microsystems for chemical analysis (μTAS) based on LTCC, polymer and IC technologies, microfluidic platforms for the synthesis of nanomaterials and optical and electrochemical microsensors. Most of these developments were applied in the environmental and industrial control fields.

Mar Puyol completed her Ph.D. in Analytical Chemistry in 2002 from the Autonomous University of Barcelona. She was working as a researcher for two years in the Applied Physics Department of the Universidad de Zaragoza until 2006. She is author of more than 40 papers related on the field. Her research interests include the study and characterization of new chromo(fluoro)ionophores and its integration as recognition elements in miniaturized optochemical sensors, the development of microsystems for chemical analysis (μTAS) based on LTCC, polymer and IC technologies and its application in environmental, agri-food, space and biomedical fields, and the design and fabrication of microfluidic platforms for the synthesis of nanomaterials and for the development of (bio) chemical miniaturized analyzers based on the use of nanostructured materials.